Journal of Inflammation Research

Dovepress
Taylor & Francis Group

Open Access Full Text Article

ORIGINAL RESEARCH

Gubi Decoction Ameliorates Porous Cartilage Endplate in an Intervertebral Disc Degeneration Model Mouse Through Inhibition of NF-κB Activity and Pyroptosis

Sai Yao[1–4,*], Yanan Li[1,3,*], Hongfeng Ruan[3,4], Lianguo Wu[1], Hanbing Zeng[1]

[1]Department of Orthopaedics, The Second Affiliated Hospital of Zhejiang Chinese Medical University, Hangzhou, Zhejiang, 310005, People's Republic of China; [2]Frontier Innovation Center, Department of Physiology and Pathophysiology, School of Basic Medical Sciences, Fudan University, Shanghai, 200032, People's Republic of China; [3]The First Clinical College of Zhejiang Chinese Medical University, Hangzhou, Zhejiang, 310053, People's Republic of China; [4]Institute of Orthopaedic and Traumatology, The First Affiliated Hospital of Zhejiang Chinese Medical University (Zhejiang Provincial Hospital of Traditional Chinese Medicine), Hangzhou, Zhejiang, 310053, People's Republic of China

*These authors contributed equally to this work

Correspondence: Lianguo Wu, Email mdwu8535@126.com; Hanbing Zeng, Email tzzhb19@163.com

Background: Intervertebral disc (IVD) degeneration (IVDD) is highly prevalent among the elderly population and stands as a leading cause of low back pain. Our prior studies have highlighted the therapeutic potential of Gubi decoction (GBD) in alleviating knee osteoarthritis, however, but the specific mechanism of GBD in treating IVDD is not clear.

Objective: To ascertain the clear mechanism of GBD for enhancing its therapeutic efficacy in treating lVDD, through comparison of its effects across different doses of GBD and clinical positive control drugs using a mouse IVDD model.

Methods: In this study, 8-week-old male mice were treated with lumbar spine instability (LSI) surgery to construct IVDD model mice. From day 3 post-LSI surgery, mice in the loxoprofen sodium tablets (LST), GBD-L, GBD-M and GBD-H groups were gavage administration with LST (23.1 mg/kg) and GBD (6.1, 12.2 and 24.4 g/kg body weight, respectively) 5 times a week for 4 and 8 weeks separately. After 8 weeks of LSI modeling, the therapeutic efficacy on IVDD was evaluated through changes in lumbar spine function, histopathological morphology, extracellular matrix (ECM) metabolism, nucleus pulposus (NP) cell viability, and cartilage endplate (CEP) cell pyroptosis; at 4 weeks after modeling, the activation of NF-κB signaling was detected.

Results: GBD can attenuate the progression of IVDD in mice, resulting in substantially increases disc height index (DHI) and NP matrix, reduced the degree of annulus fibrosus (AF) tear and the formation of cavity in CEP. In parallel, GBD significantly improved the matrix metabolism-related indexes of IVD at 8 weeks after modeling. Mechanically, GBD inhibited the expression of pyroptosis-related indicators NOD-like receptor thermal protein-domain associated protein 3 (NLRP3), cysteinyl aspartate specific-proteinase-1 (CASPASE1), gasdermin D (GSDMD), interleukin-1β (IL-1β) and interleukin-18 (IL-18) in CEP. Furthermore, GBD suppressed nuclear translocation of P65 protein, and decreased the amount of p-I-κB in CEP at 4 weeks after modeling.

Conclusion: In summary, GBD can effectively inhibit the activation of NF-κB signaling and pyroptosis of ECP, relieve the porosity of ECP, and then delay the IVDD process. GBD may serve as a potential therapeutic agent for IVDD treatment.

Keywords: GBD, pyroptosis, NF-κB signaling, IVDD

Introduction

GBD, as a tailoring prescription, derived from the Bushen Huoxue formula in *Shang Ke Da Cheng*, is one of the most important formula used in traditional Chinese medicine (TCM) and has been clinically used for long time in degenerative knee osteoarthrosis treatment.[1] The prescription consists of seven herbs: Shu Dihuang (Radix Rehmanniae Preparata), Du

Received: 25 September 2024
Accepted: 5 February 2025
Published: 18 April 2025

Graphical Abstract

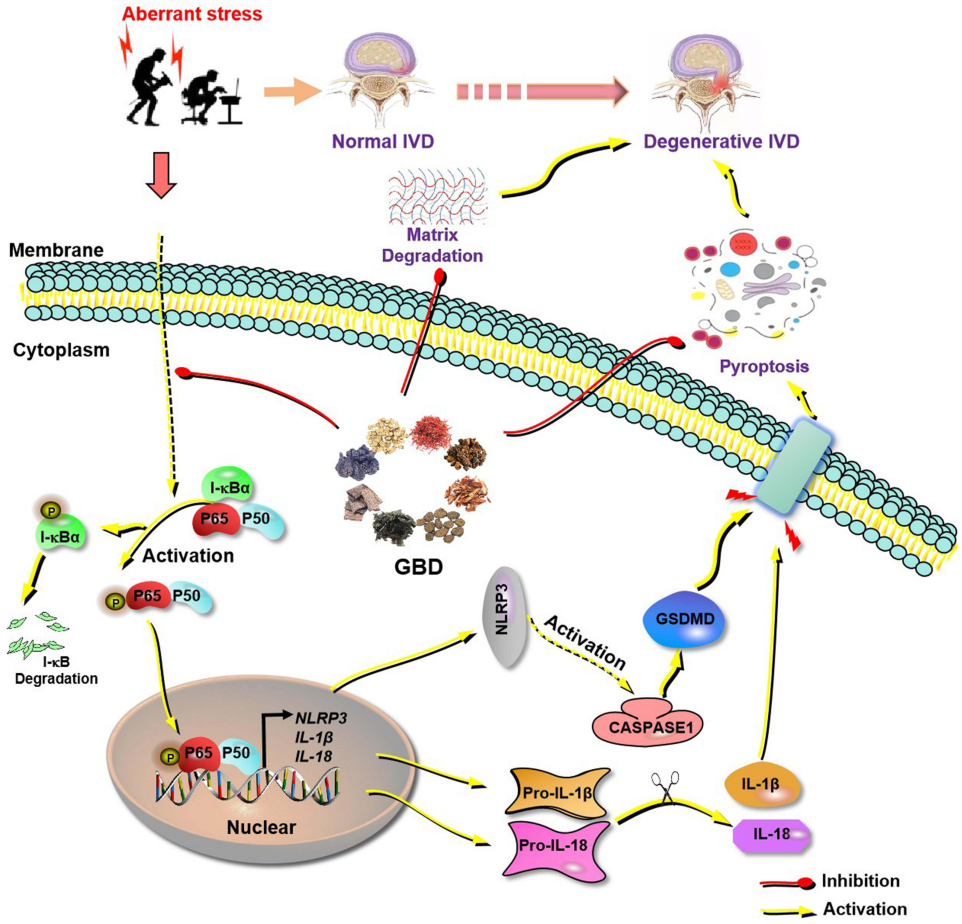

Zhong (Eucommiae Cortex), Mo Yao (Myrrha), Hong Hua (Carthami Flos), Ying Yanghuo (Herba Epimedii), Chuan Niuxi (Radix Cyathulae), and Wu Shaoshe (Zaocys dhumnades), and has the functions of tonifying kidney, strengthening bones, promoting blood circulation and dredging collaterals. However, the potential mechanism of GBD in the treatment of IVDD has not been completely determined. Several studies have shown that the Bushen Huoxue formula exhibits various biological effects, including neuroprotective, and cardioprotective effects, along with anti-inflammatory,[2] anti-oxidative, anti-pyroptosis, pro-angiogenesis[3] and pro-osteogenic differentiation activities.[4] As a tailoring prescription for Bushen Huoxue formula, we suggest that the anti-inflammatory properties of the formula may indicate a potential beneficial effect on IVDD treatment.

The IVD is composed of NP, AF, and CEP, with NP in the center, it is a proteoglycan-rich hydrophilic gel-like ECM composed mainly of type II collagen and proteoglycans, which are surrounded by a thin sheet of concentric collagen rings composed of type I fibers.[5] CEP is permeable through a thin layer bright cartilage fixes the upper and lower discs to the bony endplate of adjacent discs.[6] IVDD is a chronic process, including a progressive reduction of proteoglycan and hydration in NPs, fiber ring tears, and accompanied by sustainable mechanical unstability and loss of shock absorber function, which subsequently leads to osteophyte formation and restrict the movement of the spine.[7] IVDD is characterized by fissure formation of the AF, decreased water in the IVD, decreased elasticity, narrowing of the intervertebral space, and edema, fatation, or sclerosis of the subplated bone.[8] Typically, IVDD occurs due to the ECM is stronger in catabolism than anabolism. An important pathologic feature of IVDD is the presence of pro-inflammatory mediators[9] and

the progressive loss of the number of active NP or AF cells, ECM as well as altering the phenotype of normal IVD cells.[10] In addition, many factors can induce the abnormality of CEP, including oxidative stress,[11] apoptosis,[12] inflammation,[13,14] etc. Ectopic ossification and porosity of CEP are basic phenotypes in the process of IVDD and aging.[15,16] CEP degeneration is thought to begin with abnormal calcification,[17] a process where calcium crystals salts are deposited into pores of CEP. The calcified CEP undergoes ossification and are eventually replaced with bone.[18,19] The progressive appearance of porosity in CEP is a basic factor to induce IVDD.[15]

Pyroptosis is a new programmed form of cell death characterized by its dependence on CASPASE1 and the release of a large number of pro-inflammatory factors.[20] The NLRP3 inflammasome is a key factor in pyroptosis containing the sensor molecule NLRP3, adaptor apoptosis associated speck-like protein containing a CARD (ASC), and the effector protease CASPASE1. In the presence of inflammation, NLRP3 is activated by transcriptional translation, and ASCs are recruited through interactions, which allow ASCs to assemble into large speckle structures, after which ASCs recruit pro-CASPASE1 through interactions and hydrolyze them into active CASPASE1, which is made by active CASPASE1, which in turn cleaves pro-IL-1β and pro-IL-18 into IL-1β and IL-18. Then, IL-1β and IL-18 can combine with IL-1βR and IL-18R to mediate inflammation, Gasdermin D (GSDMD) can also be cleaved by CASPASE1 and induce pyroptosis.[21] To date, there is limited literature on the involvement of NLRP3 in the pathogenesis of IVDD and its potential uses. Studies have shown that NLRP3 inflammasomes are involved in the pathogenesis of IVDD,[22,23] However, it is not known whether GBD prevents IVDD by inhibiting pyroptosis.

It is widely accepted that the NF-κB signaling pathway plays a strong role in the multiple inflammatory responses of the many diseases, which is composed of receptors and receptor proximal signal adaptor proteins, IκB kinase complexes, IκB proteins, and NF-κB dimers.[24,25] When cells are subjected to various intracellular and extracellular stimuli, IκB kinase is activated, resulting in phosphorylation and ubiquitination of IκB protein, followed by degradation of IκB protein and release of NF-κB dimer.[26] NF-κB dimers are further activated through various post-translational modifications and transferred to the nucleus. In the nucleus, it binds to the gene of interest to facilitate transcription of the gene of interest. For example, matrix metalloproteinase 13 (MMP13) and ADAM metallopeptidase with thrombospondin type 1 motif 5 (ADAMTS-5), etc.[27] Due to its close relationship with chondrocytes, including IVDs, NF-κB signaling has been identified as a prospective target.[28] At the same time, NF-κB signaling is also an upstream activator of NLRP3 inflammasome, which initiates pyroptosis by regulating the expression of inflammasomes.[29]

At present, the correlation between GBD and IVDD treatment has not been reported, but our team has long used GBD to treat knee osteoarthritis in clinical patients, and its efficacy and safety have been recognized. Based on the great similarity in the pathogenesis of osteoarthritis, we studied the relationship between GBD and IVDD for the first time from the perspective of expanding the indications of drugs in the way of "old drugs are used for new purposes". In this study, we found that GBD has a protective effect on IVDD model mouse by attenuating cartilage degradation and inhibiting chondrocyte pyroptosis through inhibition of NF-κB signaling.

Materials and Methods

Chemicals and Reagent

Primary antibodies against phospho-NF-κB P65/RELA (Ser276) (p-P65, Cat# RLP0187), and Collagen II/COL2A1 (COL II, Cat# RLT1022) were from Ruiying Biotechnology Co., Ltd. Primary antibodies against CASPASE1 (Cat# 22915-1-AP) were obtained from Proteintech Co., Ltd. Primary antibodies against IL-1β (Cat# bs-6319R) and IL-18 (Cat# bs-0529R) were provided by Bioss. Primary antibodies against Aggrecan (AGC) (Cat# ab186414), ADAMTS-5 (Cat# ab231595), GSDMD (Cat# ab219800), MMP13 (Cat# ab219620) were ordered from Abcam. Immunohistochemical kit (Cat# PV-9001) was purchased from Zhongshan Golden Bridge Biotechnology Co., Ltd. (China) and Dylight 488 conjugated Goat Anti Rabbit IgG (Cat# RS23220) was from Immunoway. GBD was purchased from the Second Clinical Medical College of Zhejiang Chinese Medical University (Hangzhou, China) and was authenticated by the authors. LST was purchased from LEAD CHEMICAL CO., LTD (Shanghai, China) and a voucher specimen has been deposited at The Second Affiliated Hospital of Zhejiang Chinese Medical University (Hangzhou, China). Unless otherwise indicated, all other biochemicals and chemicals were supplied by Sigma-Aldrich (St. Louis, MO, USA).

Mice and IVDD Model

Seventy-two male C57BL/6J mice (8 weeks old, weighing 22 ± 2 g) were provided by the Animal Experimental Center of Zhejiang University of Traditional Chinese Medicine (SPF grade, SCXK (Shanghai): 2021–0012). All mice were kept in animal care facilities without specific pathogens, and were placed in a room at 23°C ± 2°C, with a light/dark cycle of 12–12 hours. All experimental schemes were approved by the Animal Experimental Ethics Committee of Zhejiang University of Traditional Chinese Medicine (IACUC-20230508-20). They are in accordance with the guidelines of the Asian Federation of Laboratory Animal Science Associations and the National Regulations for the Administration of Affairs Concerning Experimental Animals. All investigations complied to the principles of the Declaration of Helsinki.

The mouse IVDD model induced by LSI surgery was established as described previously.[30] In short, mice were anesthetized with isoflurane and prone on the operating table make a longitudinal incision along the dorsal midline to separate the posterior para vertebral muscles adjacent to L3~L5 vertebrae and expose the lumbar vertebrae. The spinous process, supraspinous ligament and interspinous ligament in L3~L5 segments were removed. The Sham operation group (placebo operation) is a Sham operation intervention, which omits the key steps of the IVDD model. Therefore, the mice in the sham operation group only received the operation to separate the para vertebral posterior muscles from L3~L5 vertebrae.

Experimental Design and Treatments

All mice were divided into groups according to the random number table method and intervened according to the single blind method. These mice were divided into six groups (n=12 per group): Sham group, Model group (LSI), GBD-L, GBD-M, GBD-H and LST group. All mice except those in the Sham group underwent IVDD modeling. From day 3 post-LSI surgery, mice in the LST, GBD-L, GBD-M and GBD-H. LST group were gavaged with LST (as a positive control drug, 23. 1 mg/kg) and GBD (6.1, 12.2 and 24.4 g/kg body weight, respectively) 5 times a week for 8 weeks separately. Animals were sacrificed by cervical dislocation at 4-week or 8-week post LSI surgery and the L3~L5 vertebrae of mice were collected for further evaluation the severity of IVDD.

Micro-CT (μCT) Analysis

Before histological treatment, we first evaluated paraformaldehyde (PFA) fixed vertebrae by μCT analysis, as mentioned above.[31,32] By using high-resolution μCT (SkyScan 1176; Bruker μCT, Kontich, Belgium) scanned the vertebrae with a resolution of 9 μm using a 90 kV source and a current of 300 μA. Setting of main scanning parameters: Source Voltage (kV)= 45; Source Current (uA)= 500; Filter=Al 0.2 mm; Exposure (ms)=750; Rotation Step (deg)=0.300; Angular Step (deg)=0.3000; Smoothing=2. The 3D model visualization software CTVol v2.0 (SkyScan company, San Jose, ca, USA) was used to analyze the parameters of L4~L5 IVD, and the L4~L5 vertebrae were half height. In order to quantify the IVD space, we used Image Pro Plus 4.5 (Media Cybernetics, Silver Spring, USA) to measure the distance between L4 and L5 from μCT images. Describe the TV of L5 vertebral body to calculate the medial septum except cortical bone, transverse process and spinous process. Three-dimensional structural parameters analysis includes: bone mineral density (BMD), trabecular number (Tb. N), trabecular thickness (Tb. Th), trabecular separation (Tb. Sp).

Histological Staining, Immunohistochemistry (IHC) and Immunofluorescence (IF)

The tissues were fixed in 4% buffered PFA for 72 h, decalcifed in 14% EDTA (pH 7.2~7.4) for 3 weeks at room temperature, dehydrated and then embedded in paraffin. The lumbar tissues were processed into 5 μm thick coronal-oriented sections for hematoxylin–eosin (H&E) staining. Briefly, sections were incubated with primary antibodies to AGC (1:300, Abcam, Cambridge, UK), COL II (1:500, Ruiying biological, Suzhou, China), MMP13 (1:300, Ruiying biological, Suzhou, China), ADAMTS-5 (1:300, Abcam, Cambridge, UK), NLRP3 (1:800, Proteintech, Wuhan, China), CASPASE1 (1:300, Proteintech, Wuhan, China), GSDMD (1:500, Abcam, USA), IL-1β (1:800, Bioss, Woburn, MA, USA), and IL-18 (1:400, Ruiying biological, Suzhou, China) at 4°C overnight. For IHC staining, a horseradish peroxidase streptavidin detection system (ZSGB-BIO, Beijing, China) was subsequently used to detect the immunoactivity, followed by counter staining with hematoxylin (Sigma-Aldrich, St. Louis, MO, USA). For IF analysis, the slides

were incubated with secondary antibodies conjugated with fluorescence at room temperature for 1 h. The morphometric study was performed using the Image Analysis System (Olympus, Japan). Triplicates of each sample were used for staining.

Quantitative histomorphometric analysis was conducted in a blinded manner with Image-Pro Plus Software version 6.0 (Media Cybernetics Inc, Rockville, Maryland, USA) as we previously described. Histological score was graded in a blind fashion using the definition established by Norcross et al, with some modification stological.

Rearing Frequency Test

The 5-minute rearing test was conducted to assess the rearing ability of mice, serving as an indirect indicator of lumbar discomfort. Before the formal testing, mice were acclimated to the experimental environment for at least 30 minutes. Each mouse was then gently placed into a 2 L breathable glass jar, with a camera positioned directly overhead to record its behavior. The experiment was programmed using the Smartv3.0 system, which included a 15-minute acclimation period followed by a 5-minute continuous recording of rearing behaviors. During the test, the frequency of rearing behaviors observed in the open field setup was carefully documented. To maintain objectivity, a single-blind protocol was implemented. After each test, the mouse was returned to its cage, and the open field area was thoroughly sanitized using 75% alcohol to remove any residual excreta or odors from the prior animal. This procedure ensured that subsequent tests were unaffected by lingering traces and that the environment remained dry. The same protocol was applied consistently for all test subjects.

TWL Test

Behavioral tests were performed under rigorously controlled conditions of room temperature and humidity within enclosed chambers fitted with raised metal mesh floors. Heat hyperalgesia was evaluated by measuring the TWL, which quantifies the nociceptive response to a thermal stimulus. Following a 30-minute acclimation period, each mouse was placed on the glass platform of a Hargreaves apparatus. A radiant heat source was applied to the plantar surface of the hind paw, and the latency to a withdrawal response—such as paw withdrawal, licking, or lifting—was recorded. All behavioral assessments were conducted using a blinded protocol to ensure the accuracy and impartiality of the results.

Gait Analysis

Gait analysis was performed using the DigiGait imaging system to record and evaluate the gait patterns of mice in each group. Measurements were conducted at the 4 th and 8 th weeks post-surgery. To prepare for testing, mice underwent training the day prior to familiarize themselves with traversing the track. On the testing day, mice were allowed at least 30 minutes to acclimate to the experimental environment. During the test, mice freely traversed the treadmill, and each was required to complete a minimum of three valid runs. The treadmill was set to a fixed speed of 18 cm/s, and a high-speed camera positioned beneath the transparent treadmill captured the movements of the mice, specifically tracking the color patterns of their four paws.

Statistical Analysis

All numerical data were presented as means ± SD. The statistical analysis was performed using GraphPad Prism software (San Diego, CA, United States). One-way analysis of variance test was performed to compare the means among groups, and multiple comparisons were performed using the least significant difference (LSD) test. A *P*-value less than 0.05 was statistically significant.

Results

GBD Can Effectively Improve CEP Porosity in IVDD Model Mice

To investigate the effect of GBD on mouse IVDD model induced by LSI surgery, we first performed H&E staining (Figure 1A and B) 8 weeks after LSI modeling. The results showed that compared with Sham group, there were more heterotopic ossification and cavities in CEP of mice in LSI group, NP shriveled and flattened, AF cracks increased

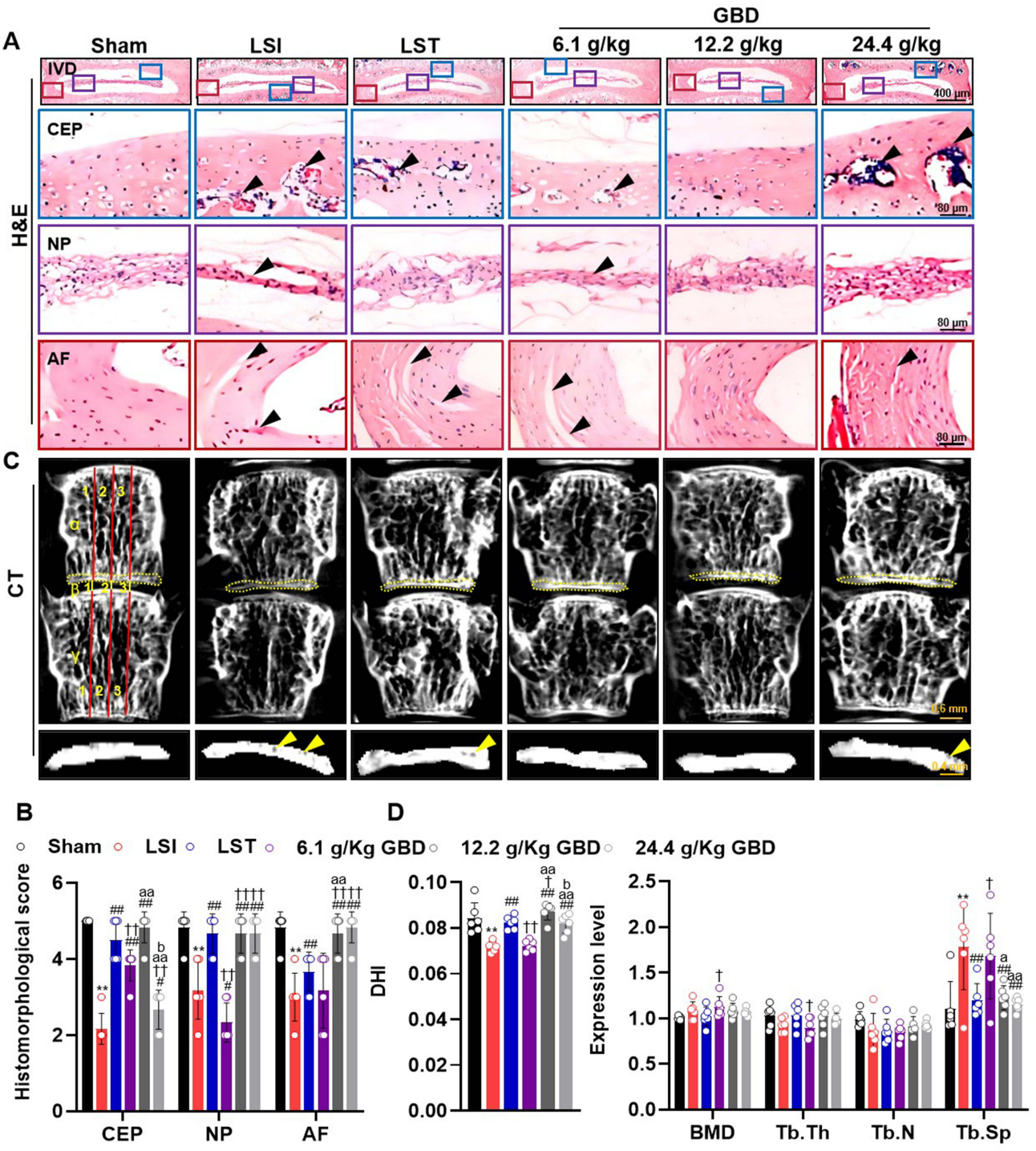

Figure 1 GBD can effectively improve the CEP porosity in IVDD model mice. From day 3 post-LSI surgery, mice in the LST, GBD-L, GBD-M and GBD-H groups were intraperitoneally injected with LST (23.1 mg/kg) and GBD (6.1, 12.2 and 24.4 g/kg body weight, respectively) 5 times a week for 8 weeks separately. H&E staining (**A**) and corresponding histomorphological scores (**B**) of IVD between L4-L5 in mice were observed after 8 weeks at post-LSI surgery. The black arrow indicates the position where the lesion appears in the process of IVDD. μCT images (**C**) and quantification of the bone morphological parameters (DHI, BMD, Tb.Th, Tb.N and Tb.Sp) (**D**) of CEP between L4~L5 in mice were observed after 8 weeks at post-LSI surgery. The DHI between the L3~L4 vertebrae was calculated based on measurements of adjacent L3~L4 vertebrae. Yellow lines represent the distances (β1~β3) between the adjacent vertebra, and red lines represent adjacent vertebral body heights (α1~α3 and γ1~γ3). DHI was calculated using the following equation: DHI=2(β1+β2+β3)/(α1+α2+α3+γ1+γ2+γ3). The yellow triangle arrow is the porous place in the CEP. The black arrow indicates the positive expression. Data are expressed as mean ± SD, **Denotes a significant difference compared with the Sham group ($^{**}P < 0.01$); # Means a significant difference compared with the LSI group ($^{\#}P < 0.05$, $^{\#\#}P < 0.01$); †Indicates a significant difference compared with the LST group ($^{\dagger}P < 0.05$, $^{\dagger\dagger}P < 0.01$); ^{a}Denotes a significant difference compared with the GBD-L group ($^{a}P < 0.05$, $^{aa}P < 0.01$); ^{b}Indicates a significant difference compared with the GYB-M group ($^{b}P < 0.05$); n = 6 per group.

Abbreviations: GBD, Gubi decoction; IVDD, intervertebral disc degeneration; LSI, lumbar spine instability; LST, loxoprofen sodium tablets; DHI, disc height index; NP, nucleus pulposus; AF, annulus fibrosus; CEP, cartilage endplate, BMD, bone mineral density; Tb. N trabecular number; Tb. Th, trabecular thickness; Tb. Sp, trabecular separation.

obviously, and the overall morphological score was worse. Compared with LSI group, LST group effectively improved ectopic ossification and cavity in CEP, and NP height increased, but the degree of AF tear was not improved obviously. In addition, we also found that compared with LSI group, low-dose and medium-dose GBD can effectively improve the degenerative phenotype of CEP and NP, while medium-dose and high-dose GBD can effectively improve the degenerative phenotype of NP and AF, and low-dose GBD has no obvious improvement on AF and high-dose GBD has no obvious improvement on CEP. Then, we detected the effect of GBD on CEP in LSI mice (Figure 1C and D) by μCT. The results showed that at the same time, we detected bone morphology-related indexes in CEP of mice, including BMD, Tb.Th, Tb.N and Tb.Sp. Compared with Sham group, LSI group showed a lower DHI score, in which LST group and GBD group with medium and high dose could effectively improve DHI of mice. In addition, compared with Sham group, the differences of BMD, Tb.Th and Tb.N in each group are not obvious, while compared with Sham group, LSI group can have larger Tb.Sp; compared with LSI group, LST group and middle and high dose GBD group all effectively improved the value of Tb.Sp.

Based on the above results, we found that GBD can effectively improve the degenerative phenotype of IVDD model mice, and the middle-dose of GBD is better.

GBD Can Effectively Improve the Matrix Degradation in IVDD Model Mice

Generally speaking, the stable matrix content maintains the physiological function of IVD. AGC and COL II are the main components in IVD tissue, and ADAMTS-5 and MMP13 are considered as the key degrading enzymes for AGC and COL II, respectively. In order to clarify the effect of GBD on matrix metabolism of LSI mice, we detected the expression of matrix metabolism indexes in IVD of mice 8 weeks after LSI modeling (Figure 2A–C). The results show that LSI group shows lower AGC content than Sham group. Compared with LSI group, LST group and middle and high dose GBD group all effectively improved the expression of AGC. Then, we detected the expression of ADAMTS-5, a proteoglycan degrading enzyme. The results showed that there was no significant difference in the expression of ADAMTS-5 in LSI group compared with Sham group. Compared with LSI group, the expression of ADAMTS-5 increased in LST group and middle and high dose GBD group, but there was no significant difference in the expression of ADAMTS-5 in middle and high dose GBD group.

At the same time, we also detected the expression of COL II in AF and CEP. The results showed that compared with Sham group, the expression of COL II in LSI group decreased, and LST and GBD groups with different doses improved the expression of COL II in AF to varying degrees. Among them, LST group and middle-dose GBD group are better than low-dose GBD group, and there is no statistical difference between them. Compared with LSI group, we also found that LST and GBD groups with different doses can improve the expression level of MMP13 in AF to varying degrees. In CEP, compared with Sham group, LSI group can reduce the expression of COL II. Compared with LSI group, LST group and middle and high dose GBD group can effectively improve the expression of COL II in CEP. However, the improvement of COL II in low-dose GBD group was not obvious. Then, we also found in CEP that the expression of MMP13 in LSI group was significantly higher than that in Sham group, while LST group and GBD group with different doses could effectively reduce the expression of MMP13 in CEP.

Based on the above results, our results show that GBD can effectively improve the matrix degradation of IVDD mice.

GBD Has No Obvious Improvement Effect on Motor Function of IVDD Model Mice

In order to clarify the effect of GBD on the motor function of LSI-induced IVDD mice, we then detected the time of 5-minute upright, TWL and gait analysis indexes [including swing time, stride length and paw area] (Figure 3A–E) at 4 th and 8 th weeks after LSI modeling. The results showed that there was no statistical difference in the functional indexes of the above groups in LSI group compared with Sham group. Compared with LSI group, LST group can effectively improve the 5-minute upright times of LSI model 4 W mice. Compared with the LST group, the low-dose GBD group can effectively reduce the 5-minute upright times of mice. Moreover, compared with the low-dose GBD group, the high-dose GBD group can improve the 5-minute upright times of mice. At 8 W after modeling, there was no statistical difference in each group.

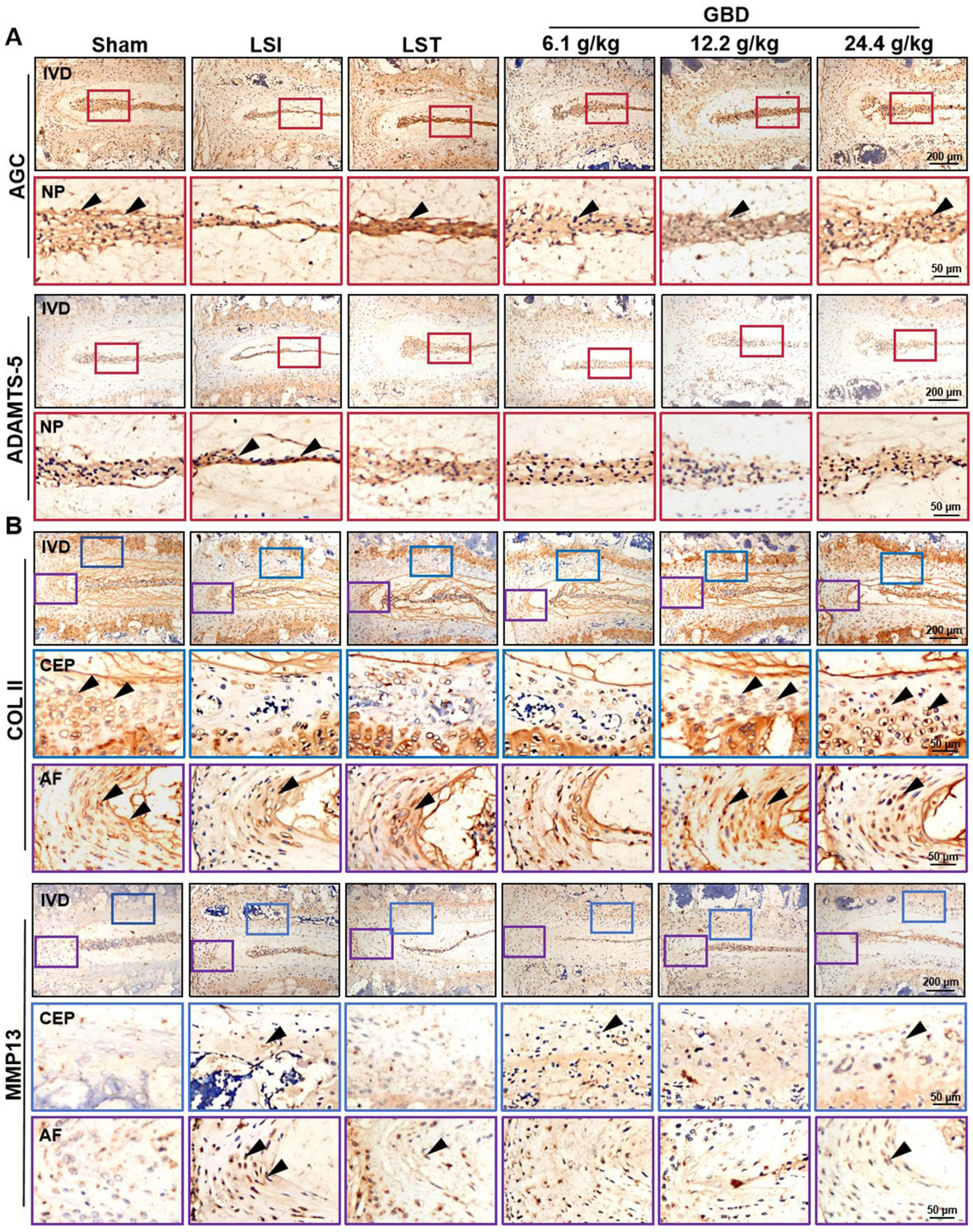

Figure 2 Continued.

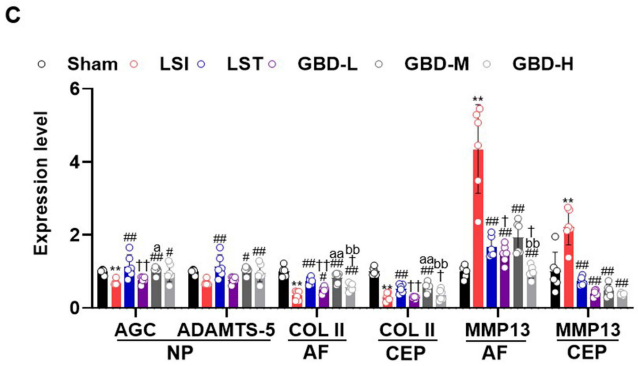

Figure 2 GBD can effectively improve the matrix degradation in IVDD model mice. (**A**–**C**) ECM components (AGC, COL II) and corresponding degrading enzymes (ADAMTS-5 and MMP13) in IVDs tissues of IVDD mice were determined by IHC analysis. The black arrow indicates the positive expression. The red box indicates NP, the purple box indicates AF and the blue box indicates CEP. Data are expressed as mean ± SD, **Denotes a significant difference compared with the Sham group (**$P < 0.01$); #Means a significant difference compared with the LSI group (#$P < 0.05$, ##$P < 0.01$); †Indicates a significant difference compared with the LST group (†$P < 0.05$, ††$P < 0.01$); aDenotes a significant difference compared with the GBD-L group (a$P < 0.05$, aa$P < 0.01$ vs); bbIndicates a significant difference compared with the GBD-M group (bb$P < 0.01$); n = 6 per group.
Abbreviations: GBD, Gubi decoction; ECM, extracellular matrix; IVD, Intervertebral disc; LSI, lumbar spine instability; LST, loxoprofen sodium tablets; NP, Nucleus pulposus; AF, annulus fibrosus; CEP, cartilage endplate; ADAMTS-5, ADAM metallopeptidase with thrombospondin type 1 motif 5; AGC, Aggrecan; COL II, Collagen II; MMP13, matrix metalloproteinase 13; IHC, Immunohistochemical.

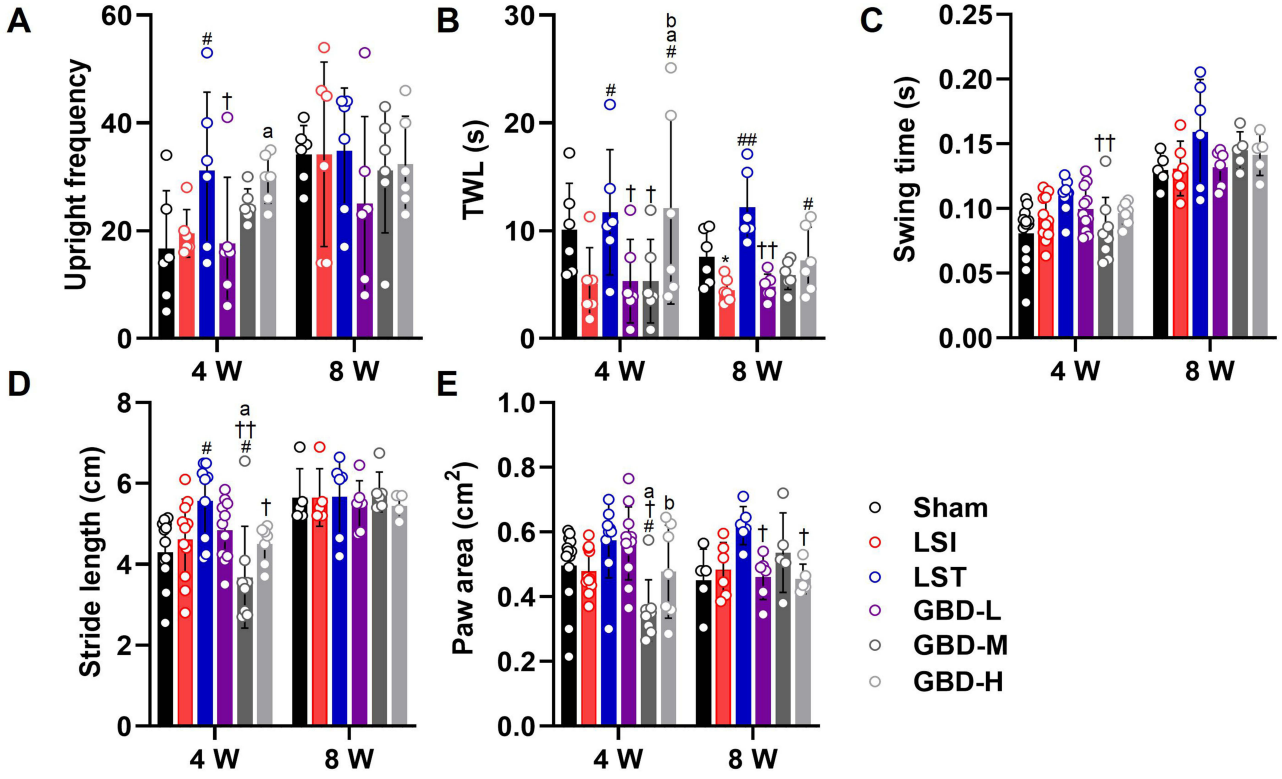

Figure 3 GBD did not significantly improve the motor function of IVDD model mice. (**A**–**E**) The behavioral test indexes including number of standing upright in 5 minutes (times), TWL (s), and gait analysis (including swing duration (ms), stride length (cm), paw area (cm^2)), were carried out in 4 and 8 weeks after the IVDD mice model. Data are expressed as mean ± SD, *Denotes a significant difference compared with the Sham group (*$P < 0.05$); #Means a significant difference compared with the LSI group (#$P < 0.05$, ##$P < 0.01$); †Indicates a significant difference compared with the LST group (†$P < 0.05$, ††$P < 0.01$); aDenotes a significant difference compared with the GBD-L group (a$P < 0.05$); bIndicates a significant difference compared with the GBD-M group (b$P < 0.05$); n = 6 per group.
Abbreviations: GBD, Gubi decoction; LSI, lumbar spine instability; LST, loxoprofen sodium tablets; TWL, thermal withdrawal latency.

https://doi.org/10.2147/JIR.S492365

At the same time, we tested the index of TWL, and the results showed that at 4 weeks after LSI modeling, compared with LSI group, LST group and high-dose GBD group, the TWL of mice could be improved. Compared with LST group, low and middle doses of GBD can reduce the threshold of heat withdrawal in mice, and there is no statistical difference between low and middle doses of GBD. However, high-dose of GBD can effectively promote the TWL in mice. 8 W after modeling, compared with Sham group, the TWL of LSI group decreased. Compared with LSI group, LST group and high-dose GBD group can promote the TWL of mice, but there is no statistical difference between low-dose and middle-dose GBD group. And compared with LST group, we found that the middle-dose group can reduce the swinging time of mice only 4 weeks after modeling. Compared with LSI group, we also found that LST group and middle-dose GBD group can promote the stride length of mice, but there is no statistical difference between low and high dose GBD group. Four weeks after LSI modeling, compared with LSI group, the middle-dose of GBD group can reduce the paw area of mice. Compared with the middle-dose GBD group, the high-dose GBD group can promote the paw area of mice during exercise. After 8 weeks, compared with the LST group, both low and high doses of GBD can reduce the paw area of mice during exercise.

Based on the above results, we conclude that GBD has no obvious improvement on the motor function on IVDD model mice.

GBD Can Effectively Alleviate the Pyroptosis Signaling in IVDD Model Mice

In order to further explore the specific mechanism of GBD effectively improving LSI-induced IVDD mice, previous studies also found that pyroptosis signaling were involved in a variety of degenerative diseases of bone and joint, so we speculated that GBD might be effective in the pyroptosis index of IVDD mice. Then, 8 W after LSI modeling, we detected the related indexes of pyroptosis pathway, including NLRP3, CASPASE1, GSDMD, IL-1β and IL-18 (Figure 4A and B). The results show that compared with Sham group, a series of pyroptosis indicators can be activated in CEP in LSI group. Compared with LSI group, LST group and different doses of GBD can improve the index of pyroptosis in CEP, and the overall effect of middle dose GBD group is the best. In terms of inhibiting the expression of NLRP3, we found that only the middle dose of GBD group was better than that of LST group, while the low and high dose of GBD group was weaker than that of LST group. Compared with LSI group, the expressions of CASPASE1, GSDMD and IL-1β were decreased in LST group and GBD group with different doses, but there was no statistical difference among different doses. Compared with LSI group, only the middle and high dose of GBD can effectively improve the expression of IL-18, and there is no statistical difference between them. Based on this, we found that the activation of pyroptosis signaling can appear in IVDD mice induced by LSI, and GBD can effectively inhibit the activation of pyroptosis signaling, and the middle-dose of GBD group is the best.

GBD Can Effectively Inhibit the NF-κB Signaling in IVDD Model Mice

To confirm whether the protective effects of GBD on OA are related to its regulation of NF-κB signaling in IVD in the LSI model, we analyzed the location of P65, p-P65 and protein levels of p-IκBα, IκBα by IF (Figure 5A). The results showed that a significant increase in nuclear translocation of P65 and p-P65 protein was observed in LSI group and GBD suppressed nuclear translocation of P65 and p-P65 protein. As can be seen from the pictures and statistics, p-P65 and p-IκBα increased after LSI surgery, and decreased significantly after GBD-M, compared to taking LST, GBD-L and GBD-H (Figure 5B). The ratio of p-IκBα/IκB and p-P65/P65 indicates the degree of activation of the NF-κB signaling pathway, and in general, the higher the ratio, the higher the degree of pathway activation. It can be seen that GBD-M has the lowest degree of activation, which means that GBD-M effectively inhibits the NF-κB signaling pathway. Taken together, these results suggest that GBD-M is a potent suppressor of NF-κB activity in chondrocytes during IVDD development.

Discussion

In the present study, we have investigated the effect of GBD on IVDD in LSI-induced IVDD murine model. We also have observed in NF-κB signaling mechanism through IVDD model mice. Our data provided molecular evidences that GBD decelerates IVDD performed as a pyroptosis inhibitor via regulation of NF-κB signaling.

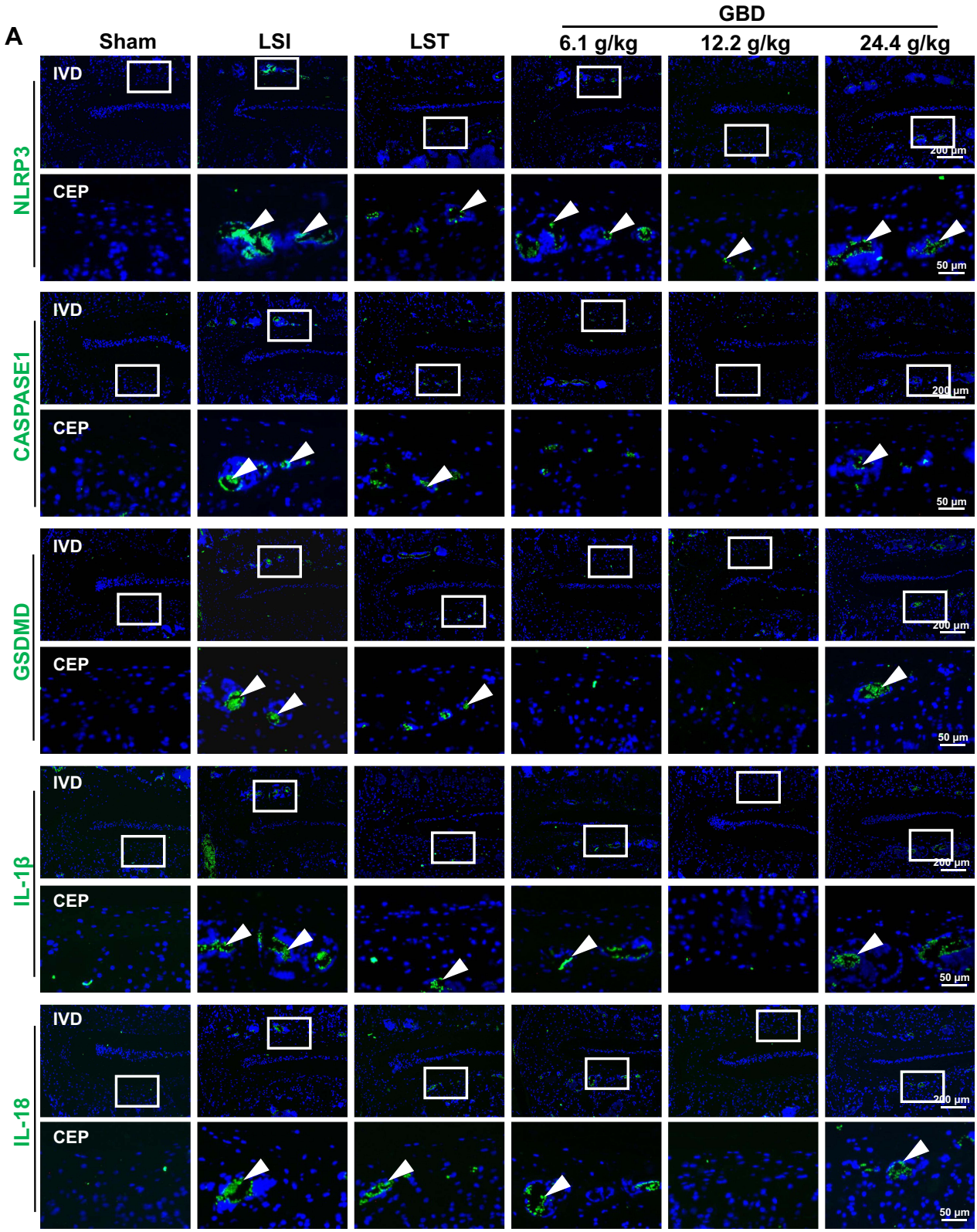

Figure 4 Continued.

https://doi.org/10.2147/JIR.S492365

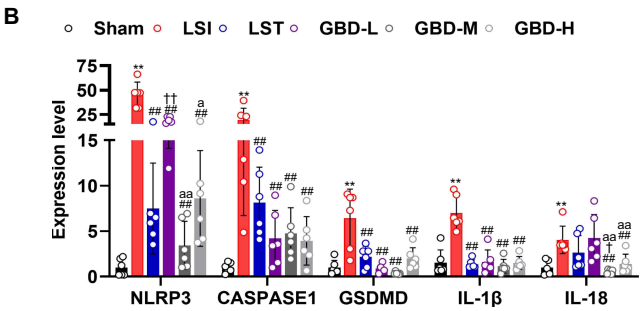

Figure 4 GBD can effectively alleviate the pyroptosis signaling in IVDD model mice. (**A**) Pyroptosis pathway indicators (NLRP3, CASPASE1, GSDMD, IL-1β and IL-18) were determined by IF staining and their statistical analysis of relative expression levels (**B**) were calculated in the CEP between L4~L5 in mice after 8 weeks at post-LSI surgery. The white arrow indicates the positive expression. The white box indicates CEP. Data are expressed as mean ± SD, **Denotes a significant difference compared with the Sham group (**$P < 0.01$); $^{\#}$Means a significant difference compared with the LSI group ($^{\#\#}P < 0.01$); †Indicates a significant difference compared with the LST group ($^{\dagger}P < 0.05$, $^{\dagger\dagger}P < 0.01$); ^{a}Denotes a significant difference compared with the GBD-L group ($^{a}P < 0.05$, $^{aa}P < 0.01$); n = 6 per group.

Abbreviations: GBD, Gubi decoction; LSI, lumbar spine instability; LST, loxoprofen sodium tablets; NLRP3, NOD-like receptor thermal protein-domain associated protein 3; CASPASE1, cysteinyl aspartate specific-proteinase-1; GSDMD, gasdermin D; 1L-1β, Interleukin-1β; 1L-18, Interleukin-18; IVD, intervertebral disc; CEP, cartilage endplate. The white box indicates CEP.

Reproducing characteristics of IVDD in animals is critical to have a better understanding of disease mechanism. LSI surgical model is one of the most common models of IVDD in laboratory animals, and strongly associated with clinical process. IVDD model provided extremely good reproducibility and considered to be a gold standard in the field.[33,34] Histology demonstrated the matrix content of NP decreased, and the formation of AF tearing and heterotopic ossification of CEP increased developed 8 weeks after surgery.[30,35–37] Consistent with the previous studies,[30,35–37] IVDD-induced mice in our research exhibited remarkable a significant decrease in height of discs, vacuole sizes in NP, ectopic bone formation in CEP, accompanied by fissures and folds in the interlamellar of AF tissues 8-weeks post-surgery, indicating the success of model establishment.

IVDD is a complicated and multifactorial process, including the increase of inflammatory cytokines, the degradation of ECM and the loss of hydrophilic matrix molecules, structural and biomechanical changes, inward growth of nerves and the release of pain factors. At present, targeting common inflammatory factors and inflammation-related signaling pathways is still an effective means to treat and delay IVDD.[38] Previous studies have demonstrated that excessive accumulation of abnormal stress accelerates the activation of IVDD process and up-regulated pyroptosis.[30,39] Consistent with the previous research, we also found that pyroptosis can be activated 8 weeks in mouse CEP after LSI modeling. Several studies have confirmed that a significant increase in the expression of pyroptosis-related proteins, such as NLRP3, CASPASE-1, and GSDMD in IVD cells of IVDD patients and murine IVDD model.[30,40] Moreover, other in vitro experiments demonstrated that exogenous stimuli, including LPS and H_2O_2, could induce inflammatory responses and degenerative phenotype of NP cells by activating NLRP3.[41,42] Interestingly, the previous studies mainly focused on NP cell pyroptosis. The difference is that our study found that the phenotype of pyroptosis induced by LSI surgery mainly focused on CEP. From the CT results, it can be seen that LSI surgery increased the Tb.Sp of CEP, which may be related to the increased expression of pyroptosis in CEP.

Chinese medicine acts as the promising alternative medicine as a therapeutic option for IVDD and might be easily accepted by clinicians and patients. GBD, as a common prescription for the treatment of degenerative knee joint diseases, is widely used in clinic because of its remarkable curative effect and safety. The composition of GBD skillfully combines the therapeutic principles of nursing vitality (tonifying Qi), promoting blood circulation, removing blood stasis, and dredging collaterals. In the prescription, Radix Rehmanniae Preparata tonifies kidney yin, tonifies essence and fills marrow; epimedium tonifies kidney yang, strengthens tendons and bones; carthamus tinctorius, myrrha and zaocys dhumnades promote blood circulation, dredge collaterals, relieve arthralgia and relieve pain. Zaocys dhumnades is also used to promote blood circulation, remove blood stasis and dredge collaterals. Early clinical investigation confirmed that GBD can effectively relieve the pain of patients, improve the activity function of knee joint, and significantly inhibit the objective indexes such as TNF-α and IL-1β. However, the precise molecular mechanisms of GBD against IVDD pathogenesis remain unclear.

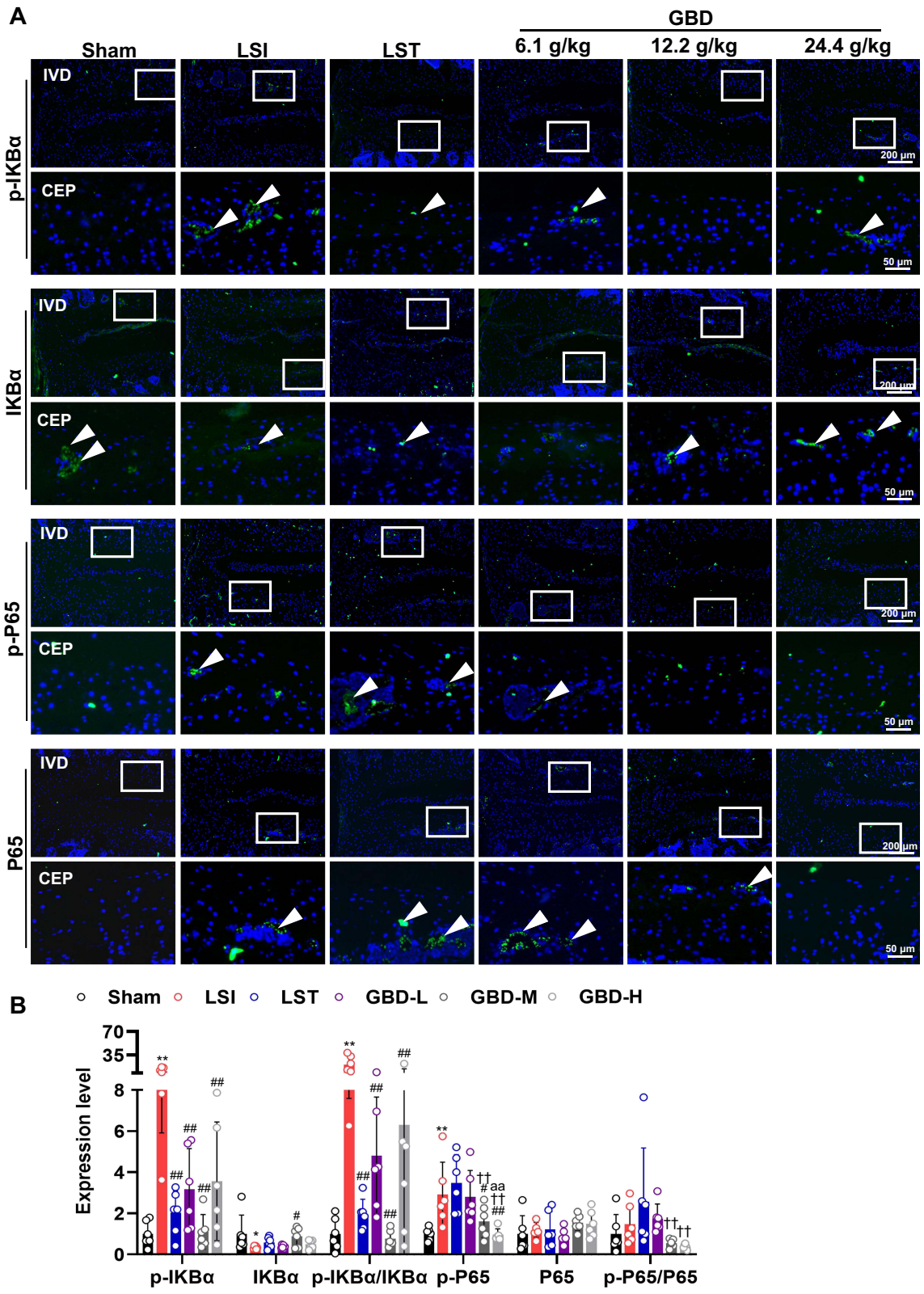

Figure 5 GBD can effectively inhibit the NF-κB signaling in IVDD model mice. NF-κB signaling indicators (p-IκBα, IκBα, p-P65 and P65) (**A**) were determined by IF staining and their statistical analysis of relative expression levels (**B**) were calculated in the CEP between L4~L5 in mice after 4 weeks at post-LSI surgery. The white box indicates CEP. The white arrow indicates the positive expression. Data are expressed as mean ± SD, *Denotes a significant difference compared with the Sham group ($^{*}P < 0.05$, $^{**}P < 0.01$); $^{\#}$Means a significant difference compared with the LSI group ($^{\#}P < 0.05$, $^{\#\#}P < 0.01$); †Indicates a significant difference compared with the LST group ($^{\dagger\dagger}P < 0.01$); ^{aa}Denotes a significant difference compared with the GBD-L group ($^{aa}P < 0.01$); n = 6 per group.

Abbreviations: GBD, Gubi decoction; LSI, lumbar spine instability; LST, loxoprofen sodium tablets; IVD, intervertebral disc; CEP, cartilage endplate.

https://doi.org/10.2147/JIR.S492365

In our study, GBD also suppressed the inflammatory reaction by decreasing the release of inflammatory cytokines (IL-1β and IL-18). Combining biochemical methods with IVDD models, we found that GBD had a protective effect on the IVD in the IVDD models, which is consistent with previous findings that kidney-tonifying and blood-activating traditional Chinese medicine can effectively alleviate the progression of IVDD. GBD not only exerts its role in protecting the IVD by reversing the height of the IVD, reducing the porosity of CEP, and reducing the matrix degradation and the index of pyroptosis 8 weeks after LSI modeling, and further mechanism study also found that the GBD can suppress NF-κB signal 4 W after modeling including a reduction in the phosphorylation status of IκB, which subsequently leads to the expression of nuclear p65.

Moreover, LST, as a commonly used anti-inflammatory and analgesic drug in clinic, is currently applicable to rheumatoid arthritis, osteoarthritis, lumbago, periarthritis of shoulder, neck-shoulder-wrist syndrome and so on. This study also discovered that the therapeutic effect of medium-dose GBD on CEP was significantly better than that of LST group and low and high dose GBD treatment group. Similarly, the mechanism of some commonly used western medicines in clinic to improve low back pain is also focused on the transformation process from ossified area of CEP to porous endplate. For example, Peng Xue et al found that low dose of celecoxib can maintain the expression level of PGE 2 in LSI-induced IVDD model, thus maintaining the intraosseous receptor mediated by PGE2/EP4 to reduce the porosity of cartilage endplate and relieve low back pain.[32] However, there is no statistical difference in some experimental results of evaluating the behavior of low back pain in this study, so it is necessary to extend the observation time later. In addition, GBD, as a decoction for tonifying kidney and promoting blood circulation, has the effect of improving IVDD compared with many other prescriptions, but it plays a different role. For example, our previous study found that Liuwei Dihuang decoction (LWDHD) can inhibit pyroptosis but mainly delay the degeneration of NP and AF, but it has no effect on the transformation of CEP from ossification to porosity.[37] This also shows that some traditional Chinese medicines with similar functions still have great differences in the actual position of action. Our team has recently identified several key components of GBD through UPLC-MS/MS analysis, including *pinoresinol diglucoside, rehmannioside D, hesperidin, liquiritin, baohuoside I, glycyrrhizic acid, kaempferol, and tangeretin*.[1] Later, we will make a comprehensive comparative study based on these monomers to clarify the key monomer of the transformation from ossified area to porous of CEP, and further clarify the exact mechanism of this monomer to delay porous CEP. Overall, our data show that GBD plays a unique role in improving porous CEP.

In recent years, numerous evidence have indicated that the NF-κB signaling pathway is pivotal in immune and inflammatory responses regulation.[43] In IVDD, it is linked to inflammation and pain propagation.[44] Our study highlights GBD's impact on this pathway, offering novel therapeutic insights inhibition of IκBα phosphorylation: IκBα restrains NF-κB in the cytoplasm. Its phosphorylation leads to degradation, releasing NF-κB for nuclear translocation and pro-inflammatory gene transcription. GBD's reduction of IκBα phosphorylation prevents NF-κB activation and translocation, thereby reducing inflammatory mediators' transcription.[45] P65, is vital for NF-κB target gene transcription, becomes more active upon phosphorylation. GBD's reduction of p-P65 levels directly suppresses NF-κB transcriptional activity, decreasing pro-inflammatory cytokines and enzymes.[46]

GBD inhibits NF-κB activation, potentially lowering cytokines, chemokines, and enzymes involved in the inflammatory process. This lessens the inflammatory environment, alleviating pain and possibly slowing IVDD progression. GBD's modulation of NF-κB could protect disc cells, prevent pyroptosis, and support a viable cellular environment in IVDD. GBD's NF-κB pathway inhibition suggests a novel, effective IVDD treatment approach. It offers therapeutic benefits over traditional anti-inflammatories by targeting a crucial pathway in the IVDD inflammatory cascade. This strategy could lead to more sustained, effective inflammation in IVDD. GBD's NF-κB inhibition provides a molecular basis for its anti-inflammatory properties in IVDD treatment. Along with its potential to modulate pyroptosis and inflammation, GBD emerges as a promising therapeutic candidate for IVDD. Further research and clinical trials are necessary to fully understand and validate GBD's clinical benefits in IVDD patients, and especially the potential of targeting NF-κB signaling pathway to treat IVDD. In addition, GBD, as a new use of old drugs, not only provides a treatment choice for patients with knee osteoarthritis, but also provides a treatment method for patients with IVDD. In the future, with the application of artificial intelligence and big data technology, the potential of new use of old drugs will be

further tapped. Although the new use of old drugs has great potential, there are still some challenges: the dosage of drug intervention varies from disease to disease, and the side effects of drugs need further careful consideration.

At the same time, this experiment also has several shortcomings, first of all, in terms of motor function detection, we used a series of indicators related to IVDs including number of standing upright in 5 minutes, TWL, and gait analysis (including swing duration, stride length and paw area). However, the results showed that there was no obvious correlation in total movement change, on the one hand, because the randomness of the experimental animals was relatively large, and the fact that these indicators did not have a definite relationship with the IVD. Secondly, in terms of drug dosage, the results showed that the treatment effect of medium-dose GBD was the best, which also needs to be further studied to explore the optimal dosage in IVDD patients. Then, although the relationship between NF-κB and pyroptosis was not confirmed in this experiment, some experiments have confirmed that NF-κB is the upstream signaling pathway of pyroptosis.[47,48] Finally, there was no significant difference between the treatment and IVDD model groups on μCT, which may be a combined action of CEP porosity and CEP sclerosis,[49] the dynamic changes between heterotopic ossification and porosity of CEP in IVDD process still needs further experimental study.

Conclusions

In conclusion, we found that GBD ameliorated IVDD progression in IVDD model mouse. GBD attenuated cartilage degradation, inhibited chondrocyte pyroptosis via inhibition of NF-κB activation. Thus, these results uncover NF-κB inactivation and subsequent attenuation of cartilage matrix catabolism and pyroptosis of chondrocytes in articular cartilage as a hitherto uncharacterized mechanism controlling GBD-mediated preventive effect on IVDD progression. GBD's suppression of the NF-κB pathway underlines its anti-inflammatory and partial analgesic properties for IVDD treatment. Combined with its potential to regulate inflammatory, GBD emerges as a promising candidate for developing novel IVDD therapies. Further research and clinical trials are essential to fully validate GBD's clinical efficacy in IVDD, particularly its influence on the NF-κB pathway.

Abbreviation

GBD, Gubi decoction; IVD, Intervertebral disc; lVDD, Intervertebral disc degeneration; LSI, lumbar spine instability; LST, loxoprofen sodium tablets; DHI, disc height index; NP, nucleus pulposus; AF, annulus fibrosus; CEP, cartilaginous endplate; NLRP3, NOD-like receptor thermal protein–domain associated protein 3; CASPASE1, cysteinyl aspartate specific-proteinase-1; GSDMD, gasdermin D; IL-1β, Interleukin-1beta; IL-18, Interleukin-18; TCM, traditional Chinese medicine; ASC, apoptosis associated speck-like protein containing a CARD; μCT, Micro-CT; BMD, bone mineral density; Tb. N, trabecular number; Tb. Th, trabecular thickness; Tb. Sp, trabecular separation; IHC, immunohistochemistry; IF, immunofluorescence; LSD, least significant difference; TWL, thermal withdrawal latency; PFA, paraformaldehyde; ADAMTS-5, ADAM metallopeptidase with thrombospondin type 1 motif 5; AGC, Aggrecan; COL II, Collagen II; MMP13, matrix metalloproteinase 13.

Data Sharing Statement

Data will be made available on request.

Acknowledgments

We thank all animal technicians for the essential husbandry work with our animal models. We thank the national flagship project department of integrated traditional Chinese and western medicine for its strong support. We thank Dr. Zhao Meng for providing many practical opinions and suggestions in the process of revising this article.

Author Contributions

All authors made a significant contribution to the work reported, whether that is in the conception, study design, execution, acquisition of data, analysis and interpretation, or in all these areas; took part in drafting, revising or critically reviewing the article; gave final approval of the version to be published; have agreed on the journal to which the article has been submitted; and agree to be accountable for all aspects of the work.

Funding

This study was supported by grants from Zhejiang Provincial Traditional Chinese Medicine Science and Technology Program (2024ZL514), Research Project of Zhejiang Chinese Medical University (2023JKZKTS40) and National Natural Science Foundation of China (82170238).

Disclosure

The authors declare no competing interests.

References

1. Cui L, Shen G, Yu Y, et al. Gubi decoction mitigates knee osteoarthritis via promoting chondrocyte autophagy through METTL3-mediated ATG7 m (6)A methylation. *J Cell Mol Med*. 2024;28(16):e70019. doi:10.1111/jcmm.70019
2. Yuan Q, Kan WB, Song PF, Zhao J, Yu WG, Wang YJ. Influence of bushen huoxue decoction on beta-catenin, MMP-7 of synoviocytes in rats with knee osteoarthritis. *Zhongguo Gu Shang*. 2012;25(9):761–765.
3. Xie Y, Zhang J, Yang S, et al. Role of Bushen Huoxue Formula and transplanted endothelial progenitor cells play in promoting endplate microcirculation and attenuating intervertebral disc degeneration. *Heliyon*. 2024;10(6):e28095. doi:10.1016/j.heliyon.2024.e28095
4. Xia C, Zou Z, Fang L, et al. Bushenhuoxue formula promotes osteogenic differentiation of growth plate chondrocytes through β-catenin-dependent manner during osteoporosis. *Biomed Pharmacother*. 2020;127:110170. doi:10.1016/j.biopha.2020.110170
5. Kritschil R, Scott M, Sowa G, Vo N. Role of autophagy in intervertebral disc degeneration. *J Cell Physiol*. 2022;237(2):1266–1284. doi:10.1002/jcp.30631
6. Ashinsky BG, Gullbrand SE, Wang C, et al. Degeneration alters structure-function relationships at multiple length-scales and across interfaces in human intervertebral discs. *J Anat*. 2021;238(4):986–998. doi:10.1111/joa.13349
7. Yang S, Zhang Y, Peng Q, et al. Regulating pyroptosis by mesenchymal stem cells and extracellular vesicles: a promising strategy to alleviate intervertebral disc degeneration. *Biomed Pharmacother*. 2024;170:116001. doi:10.1016/j.biopha.2023.116001
8. Zhang T, Wang Y, Li R, et al. ROS-responsive magnesium-containing microspheres for antioxidative treatment of intervertebral disc degeneration. *Acta Biomater*. 2023;158:475–492. doi:10.1016/j.actbio.2023.01.020
9. Shin JH, Park S, Cho H, Kim JH, Choi H. Adipokine human Resistin promotes obesity-associated inflammatory intervertebral disc degeneration via pro-inflammatory cytokine cascade activation. *Sci Rep*. 2022;12(1):8936. doi:10.1038/s41598-022-12793-2
10. Qingxin S, Kai J, Dandan Z, et al. Programmable DNA hydrogel provides suitable microenvironment for enhancing autophagy-based therapies in intervertebral disc degeneration treatment. *J Nanobiotechnology*. 2023;21(1):350. doi:10.1186/s12951-023-02109-5
11. Kang L, Liu S, Li J, Tian Y, Xue Y, Liu X. Parkin and Nrf2 prevent oxidative stress-induced apoptosis in intervertebral endplate chondrocytes via inducing mitophagy and anti-oxidant defenses. *Life Sci*. 2020;243:117244. doi:10.1016/j.lfs.2019.117244
12. Cazzanelli P, Wuertz-Kozak K. MicroRNAs in intervertebral disc degeneration, apoptosis, inflammation, and mechanobiology. *Int J mol Sci*. 2020;21(10):3601. doi:10.3390/ijms21103601
13. Ge Q, Ying J, Shi Z, et al. Chlorogenic Acid retards cartilaginous endplate degeneration and ameliorates intervertebral disc degeneration via suppressing NF-κB signaling. *Life Sci*. 2021;274:119324. doi:10.1016/j.lfs.2021.119324
14. Tang P, Zhu R, Ji WP, et al. The NLRP3/Caspase-1/Interleukin-1β axis is active in human lumbar cartilaginous endplate degeneration. *Clin Orthop Relat Res*. 2016;474(8):1818–1826. doi:10.1007/s11999-016-4866-4
15. Rodriguez AG, Rodriguez-Soto AE, Burghardt AJ, Berven S, Majumdar S, Lotz JC. Morphology of the human vertebral endplate. *J Orthop Res*. 2012;30(2):280–287. doi:10.1002/jor.21513
16. Bian Q, Jain A, Xu X, et al. Excessive activation of TGFβ by spinal instability causes vertebral endplate sclerosis. *Sci Rep*. 2016;6:27093. doi:10.1038/srep27093
17. Roberts S, Urban JP, Evans H, Eisenstein SM. Transport properties of the human cartilage endplate in relation to its composition and calcification. *Spine*. 1996;21(4):415–420. doi:10.1097/00007632-199602150-00003
18. Moore RJ. The vertebral end-plate: what do we know. *Eur Spine J*. 2000;9(2):92–96. doi:10.1007/s005860050217
19. Wang Y, Battié MC, Boyd SK, Videman T. The osseous endplates in lumbar vertebrae: thickness, bone mineral density and their associations with age and disk degeneration. *Bone*. 2011;48(4):804–809. doi:10.1016/j.bone.2010.12.005
20. Badr G, El-Hossary FM, Lasheen F, et al. Cold atmospheric plasma induces the curing mechanism of diabetic wounds by regulating the oxidative stress mediators iNOS and NO, the pyroptotic mediators NLRP-3, Caspase-1 and IL-1β and the angiogenesis mediators VEGF and Ang-1. *Biomed Pharmacother*. 2023;169:115934. doi:10.1016/j.biopha.2023.115934
21. Luo J, Yang Y, Wang X, Chang X, Fu S. Role of pyroptosis in intervertebral disc degeneration and its therapeutic implications. *Biomolecules*. 2022;12(12):1804. doi:10.3390/biom12121804
22. Yu Y, Li W, Xian T, Tu M, Wu H, Zhang J. Human embryonic stem-cell-derived exosomes repress NLRP3 inflammasome to alleviate pyroptosis in nucleus pulposus cells by transmitting miR-302c. *Int J mol Sci*. 2023;24(8):7664. doi:10.3390/ijms24087664
23. Wang Z, Zhang P, Zhao Y, et al. Scutellarin protects against mitochondrial reactive oxygen species-dependent NLRP3 inflammasome activation to attenuate intervertebral disc degeneration. *Front Bioeng Biotechnol*. 2022;10:883118. doi:10.3389/fbioe.2022.883118
24. Liu T, Zhang L, Joo D, Sun SC. NF-κB signaling in inflammation. *Signal Transduct Target Ther*. 2017;2:17023. doi:10.1038/sigtrans.2017.23
25. Chang SH, Mori D, Kobayashi H, et al. Excessive mechanical loading promotes osteoarthritis through the gremlin-1-NF-κB pathway. *Nat Commun*. 2019;10(1):1442. doi:10.1038/s41467-019-09491-5
26. Zhang J, Zhang R, Li W, Ma XC, Qiu F, Sun CP. IκB kinase β (IKKβ): structure, transduction mechanism, biological function, and discovery of its inhibitors. *Int J Biol Sci*. 2023;19(13):4181–4203. doi:10.7150/ijbs.85158
27. Hu J, Zhou J, Wu J, et al. Loganin ameliorates cartilage degeneration and osteoarthritis development in an osteoarthritis mouse model through inhibition of NF-κB activity and pyroptosis in chondrocytes. *J Ethnopharmacol*. 2020;247:112261. doi:10.1016/j.jep.2019.112261

28. Zhang GZ, Liu MQ, Chen HW, et al. NF-κB signalling pathways in nucleus pulposus cell function and intervertebral disc degeneration. *Cell Prolif*. 2021;54(7):e13057. doi:10.1111/cpr.13057
29. Guo H, Callaway JB, Ting JP. Inflammasomes: mechanism of action, role in disease, and therapeutics. *Nat Med*. 2015;21(7):677–687. doi:10.1038/nm.3893
30. Fu F, Bao R, Yao S, et al. Aberrant spinal mechanical loading stress triggers intervertebral disc degeneration by inducing pyroptosis and nerve ingrowth. *Sci Rep*. 2021;11(1):772. doi:10.1038/s41598-020-80756-6
31. Hildebrand T, Laib A, Müller R, Dequeker J, Rüegsegger P. Direct three-dimensional morphometric analysis of human cancellous bone: microstructural data from spine, femur, iliac crest, and calcaneus. *J Bone Miner Res*. 1999;14(7):1167–1174. doi:10.1359/jbmr.1999.14.7.1167
32. Yu H, Yao S, Zhou C, et al. Morroniside attenuates apoptosis and pyroptosis of chondrocytes and ameliorates osteoarthritic development by inhibiting NF-κB signaling. *J Ethnopharmacol*. 2021;266:113447. doi:10.1016/j.jep.2020.113447
33. Ni S, Ling Z, Wang X, et al. Sensory innervation in porous endplates by Netrin-1 from osteoclasts mediates PGE2-induced spinal hypersensitivity in mice. *Nat Commun*. 2019;10(1):5643. doi:10.1038/s41467-019-13476-9
34. Fan Y, Zhang W, Huang X, et al. Senescent-like macrophages mediate angiogenesis for endplate sclerosis via IL-10 secretion in male mice. *Nat Commun*. 2024;15(1):2939. doi:10.1038/s41467-024-47317-1
35. Zhou C, Yao S, Fu F, et al. Morroniside attenuates nucleus pulposus cell senescence to alleviate intervertebral disc degeneration via inhibiting ROS-Hippo-p53 pathway. *Front Pharmacol*. 2022;13:942435. doi:10.3389/fphar.2022.942435
36. Zhang H, Yao S, Zhang Z, et al. Network pharmacology and experimental validation to reveal the pharmacological mechanisms of liuwei dihuang decoction against intervertebral disc degeneration. *Drug Des Devel Ther*. 2021;15:4911–4924. doi:10.2147/DDDT.S338439
37. Ge Y, Xie Y, Chai J, et al. Augmented Cornus officinalis levels in liuwei dihuang decoction inhibits nucleus pulposus cell pyroptosis to enhance therapeutic efficacy against intervertebral disc degeneration. *J Inflamm Res*. 2024;17:4453–4465. doi:10.2147/JIR.S465690
38. Lyu FJ, Cui H, Pan H, et al. Painful intervertebral disc degeneration and inflammation: from laboratory evidence to clinical interventions. *Bone Res*. 2021;9(1):7. doi:10.1038/s41413-020-00125-x
39. Sun K, Yan C, Dai X, et al. Catalytic nanodots-driven pyroptosis suppression in nucleus pulposus for antioxidant intervention of intervertebral disc degeneration. *Adv Mater*. 2024;36(19):e2313248. doi:10.1002/adma.202313248
40. Zhang J, Zhang J, Zhang Y, et al. Mesenchymal stem cells-derived exosomes ameliorate intervertebral disc degeneration through inhibiting pyroptosis. *J Cell Mol Med*. 2020;24(20):11742–11754. doi:10.1111/jcmm.15784
41. Song Y, Wang Y, Zhang Y, et al. Advanced glycation end products regulate anabolic and catabolic activities via NLRP3-inflammasome activation in human nucleus pulposus cells. *J Cell Mol Med*. 2017;21(7):1373–1387. doi:10.1111/jcmm.13067
42. Tian Y, Bao Z, Ji Y, Mei X, Yang H. Epigallocatechin-3-gallate protects H(2)O(2)-induced nucleus pulposus cell apoptosis and inflammation by inhibiting cGAS/Sting/NLRP3 activation. *Drug Des Devel Ther*. 2020;14:2113–2122. doi:10.2147/DDDT.S251623
43. Iacobazzi D, Convertini P, Todisco S, Santarsiero A, Iacobazzi V, Infantino V. New insights into NF-κB signaling in innate immunity: focus on immunometabolic crosstalks. *Biology*. 2023;12(6):776. doi:10.3390/biology12060776
44. Yang B, Zhang Z, Yang Z, et al. Chanling gao attenuates bone cancer pain in rats by the IKKβ/NF-κB signaling pathway. *Front Pharmacol*. 2020;11:525. doi:10.3389/fphar.2020.00525
45. Li X, Hu Y. Attribution of NF-κB activity to CHUK/IKKα-involved carcinogenesis. *Cancers*. 2021;13(6):1411. doi:10.3390/cancers13061411
46. Maimaitiaili N, Zeng Y, Ju P, et al. NLRC3 deficiency promotes hypoxia-induced pulmonary hypertension development via IKK/NF-κB p65/HIF-1α pathway. *Exp Cell Res*. 2023;431(2):113755. doi:10.1016/j.yexcr.2023.113755
47. Luo X, Bao X, Weng X, et al. The protective effect of quercetin on macrophage pyroptosis via TLR2/Myd88/NF-κB and ROS/AMPK pathway. *Life Sci*. 2022;291:120064. doi:10.1016/j.lfs.2021.120064
48. Long JX, Tian MZ, Chen XY, et al. The role of NLRP3 inflammasome-mediated pyroptosis in ischemic stroke and the intervention of traditional Chinese medicine. *Front Pharmacol*. 2023;14:1151196. doi:10.3389/fphar.2023.1151196
49. Sampson SL, Sylvia M, Fields AJ. Effects of dynamic loading on solute transport through the human cartilage endplate. *J Biomech*. 2019;83:273–279. doi:10.1016/j.jbiomech.2018.12.004